

Transverse Relaxation Time Fractal Dimension of Nuclear Magnetic Resonance for Characterizing Shajara Reservoirs of the Permo-Carboniferous Shajara Formation, Saudi Arabia

Khalid Elyas Mohamed Elameen Alkhidir

Department of petroleum and Natural Gas Engineering, College of Engineering, King Saud university, Riyadh, Saudi Arabia.

*Corresponding author

Prof. Khalid Elyas Mohamed Elameen Alkhidir, Ph.D., Department of petroleum and Natural Gas Engineering, College of Engineering, King Saud University, Riyadh, Saudi Arabia, Tel: +966114679118, E-mail: kalkhidir@ksu.edu.sa

Submitted: 03 Feb 2019; Accepted: 10 Feb 2019; Published: 21 Mar 2019

Abstract

The quality of a reservoir can be described in details by the application of transverse relaxation time of nuclear magnetic resonance fractal dimension. The objective of this research is to calculate fractal dimension from the relationship among transverse relaxation time of nuclear magnetic resonance, maximum transverse relaxation time of nuclear magnetic resonance and wetting phase saturation and to confirm it by the fractal dimension derived from the relationship among capillary pressure and wetting phase saturation. In this research, porosity was measured on real collected sandstone samples and permeability was calculated theoretically from capillary pressure profile measured by mercury intrusion techniques. Two equations for calculating the fractal dimensions have been employed. The first one describes the functional relationship between wetting phase saturation, transverse relaxation time of nuclear magnetic resonance, maximum transverse relaxation time of nuclear magnetic resonance and fractal dimension. The second equation implies to the wetting phase saturation as a function of capillary pressure and the fractal dimension. Two procedures for obtaining the fractal dimension have been developed. The first procedure was done by plotting the logarithm of the ratio between transverse relaxation time of nuclear magnetic resonance and maximum transverse relaxation time of nuclear magnetic resonance versus logarithm wetting phase saturation. The slope of the first procedure = $3-D_f$ (fractal dimension). The second procedure for obtaining the fractal dimension was completed by plotting logarithm of capillary pressure versus the logarithm of wetting phase saturation. The slope of the second procedure = $D_f - 3$. The results show similarities between transverse relaxation time of nuclear magnetic resonance and capillary pressure fractal dimension.

Keywords: Shajara Reservoirs, Shajara Formation, Transverse relaxation time of nuclear magnetic resonance fractal dimension

Introduction

Seismo electric effects related to electro kinetic potential, dielectric permittivity, pressure gradient, fluid viscosity, and electric conductivity was first reported by Frenkel J [1]. Capillary pressure follows the scaling law at low wetting phase saturation was reported by Li K, and Williams W [2]. Seismo electric phenomenon by considering electro kinetic coupling coefficient as a function of effective charge density, permeability, fluid viscosity and electric conductivity was reported by Revil A, and Jardani A [3]. The magnitude of seismo electric current depends porosity, pore size, zeta potential of the pore surfaces, and elastic properties of the matrix was investigated by Dukhin A, et al. [4]. The tangent of the ratio of converted electric field to pressure is approximately in inverse proportion to permeability was studied by Guan W, et al. [5]. Permeability inversion from seismo electric log at low frequency was studied by Hu H, et al. [6]. They reported that, the tangent of the ratio among electric excitation intensity and pressure

field is a function of porosity, fluid viscosity, frequency, tortuosity, fluid density and Dracy permeability. A decrease of seismo electric frequencies with increasing water content was reported by Borde C, et al. [7]. An increase of seismo electric transfer function with increasing water saturation was studied by Jardani A, and Revil A [8]. An increase of dynamic seismo electric transfer function with decreasing fluid conductivity was described by Holzhauser J, et al. [9]. The amplitude of seismo electric signal increases with increasing permeability which means that the seismo electric effects are directly related to the permeability and can be used to study the permeability of the reservoir was illustrated by Rong P, et al. [10]. Seismo electric coupling is frequency dependent and decreases exponentially when frequency increases was demonstrated by Djuraev U, et al. [11]. An increase of permeability with increasing pressure head and bubble pressure fractal dimension was reported by Alkhidir KEME [12]. An increase of geometric and arithmetic relaxation time of induced polarization fractal dimension with permeability increasing and grain size was described by Alkhidir KEME [13-15]. An increase of seismo electric field fractal dimension with increasing permeability

and grain size was described by Alkhidir KEME [16,17]. An increase of resistivity fractal dimension with increasing permeability and grain size was illustrated by Alkhidir KEME [18,19]. An increase of electro kinetic fractal dimension with increasing permeability and grain size was demonstrated by Alkhidir KEME [20,21]. An increase of electric potential energy with increasing permeability and grain size was defined by Alkhidir KEME [22]. An increase of electric potential gradient fractal dimension with increasing permeability and grain size was defined by Alkhidir KEME [23]. An increase of seismic time with increasing permeability and grain size was described by Alkhidir KEME [24].

Materials and Methods

The transverse relaxation time of nuclear magnetic resonance can be scaled as

$$S_w = \left[\frac{NMR_{T2}^{\frac{1}{2}}}{NMR_{T2max}^{\frac{1}{2}}} \right]^{[3-Df]} \quad 1$$

Where S_w the water saturation, NMR_{T2} transverse relaxation time of nuclear magnetic resonance in second, NMR_{T2max} maximum transverse relaxation time of nuclear magnetic resonance in second, and Df the fractal dimension.

Equation 1 can be proofed from

$$k = \left[\frac{\Phi}{2 * S_{pv}^2} \right] \quad 2$$

Where k the permeability in square meter, Φ the porosity, S_{pv} the surface area per unit pore volume in meter⁻¹.

The surface area per unit pore volume can be scaled as

$$S_{pv} = \left[\frac{1}{\rho * NMR_{T2}} \right] \quad 3$$

Where S_{pv} surface area per unit pore volume in meter⁻¹, ρ the surface relaxation in meter/second, NMR_{T2} the transverse relaxation time of nuclear magnetic resonance in second.

Insert equation 3 into equation 2

$$k = \left[\frac{\Phi * \rho^2 * NMR_{T2}^2}{2} \right] \quad 4$$

The permeability k can also be scaled as

$$k = \left[\frac{Q * \mu * l}{A * \Delta p} \right] \quad 5$$

Where k the permeability in square meter, Q the flow rate in cubic meter/second, μ the fluid viscosity in pascal*second, l the capillary length in meter, A the area in square meter, and Δ the pressure difference in pascal.

Insert equation 5 into equation 4

$$\left[\frac{Q * \mu * l}{A * \Delta p} \right] = \left[\frac{\Phi * \rho^2 * NMR_{T2}^2}{2} \right] \quad 6$$

The flow rate Q can be scaled as

$$Q = \left[\frac{3.14 * r^4 * \Delta p}{8 * \mu * l} \right] \quad 7$$

Insert equation 7 into equation 6

$$\left[\frac{3.14 * r^4 * \Delta p * \mu * l}{8 * \mu * l * A * \Delta p} \right] = \left[\frac{\Phi * \rho^2 * NMR_{T2}^2}{2} \right] \quad 8$$

Equation 8 after simplification will become

$$r^4 = \left[\frac{8 * A * \Phi * \rho^2 * NMR_{T2}^2}{3.14 * 2} \right] \quad 9$$

The maximum pore radius can be scaled as

$$r_{max}^4 = \left[\frac{8 * A * \Phi * \rho^2 * NMR_{T2max}^2}{3.14 * 2} \right] \quad 10$$

Divide equation 9 by equation 10

$$\left[\frac{r^4}{r_{max}^4} \right] = \left[\frac{\left[\frac{8 * A * \Phi * \rho^2 * NMR_{T2}^2}{3.14 * 2} \right]}{\left[\frac{8 * A * \Phi * \rho^2 * NMR_{T2max}^2}{3.14 * 2} \right]} \right] \quad 11$$

Equation 11 after simplification will become

$$\left[\frac{r^4}{r_{max}^4} \right] = \left[\frac{NMR_{T2}^2}{NMR_{T2max}^2} \right] \quad 12$$

Take the fourth root of equation 12

$$\sqrt[4]{\left[\frac{r^4}{r_{max}^4} \right]} = \sqrt[4]{\left[\frac{NMR_{T2}^2}{NMR_{T2max}^2} \right]} \quad 13$$

Equation 13 after simplification will become

$$\left[\frac{r}{r_{max}} \right] = \left[\frac{NMR_{T2}^{\frac{1}{2}}}{NMR_{T2max}^{\frac{1}{2}}} \right] \quad 14$$

Take the logarithm of equation 14

$$\log \left[\frac{r}{r_{max}} \right] = \log \left[\frac{NMR_{T2}^{\frac{1}{2}}}{NMR_{T2max}^{\frac{1}{2}}} \right] \quad 15$$

$$\text{But, } \log \left[\frac{r}{r_{max}} \right] = \left[\frac{\log S_w}{3 - Df} \right] \quad 16$$

Insert equation 16 into equation 15

$$\left[\frac{\log S_w}{3 - Df} \right] = \log \left[\frac{NMR_{T2}^{\frac{1}{2}}}{NMR_{T2max}^{\frac{1}{2}}} \right] \quad 17$$

Equation 17 after log removal will become

$$S_w = \left[\frac{\text{NMR}_{T2}^{\frac{1}{2}}}{\text{NMR}_{T2\text{max}}^{\frac{1}{2}}} \right]^{[3-Df]} \quad 18$$

Equation 18 the proof of equation 1 which relates the water saturation, transverse relaxation time of nuclear magnetic resonance, maximum transverse relaxation time of nuclear magnetic resonance, and the fractal dimension.

The capillary pressure can be scaled as

$$\log S_w = [Df - 3] * \log P_c + \text{constant} \quad 19$$

Where S_w the water saturation, Df the fractal dimensions and p_c the capillary pressure.

Results and Discussion

Based on field observation the Shajara Reservoirs of the Permo-

Carboniferous Shajara Formation were divided here into three units as described in Figure 1. These units from bottom to top are: Lower Shajara Reservoir, Middle Shajara reservoir, and Upper Shajara Reservoir. Their acquired results of the transverse relaxation time of nuclear magnetic resonance fractal dimension and capillary pressure fractal dimension are displayed in Table 1. Based on the attained results it was found that the transverse relaxation time of nuclear magnetic resonance fractal dimension is equal to the capillary pressure fractal dimension. The maximum value of the fractal dimension was found to be 2.7872 assigned to sample SJ13 from the Upper Shajara Reservoir as verified in Table 1. Whereas the minimum value of the fractal dimension 2.4379 was reported from sample SJ3 from the Lower Shajara reservoir as displayed in Table 1. The transverse relaxation time of nuclear magnetic resonance fractal dimension and capillary pressure fractal dimension was observed to increase with increasing permeability as proofed in Table 1 owing to the possibility of having interconnected channels.

Table 1 Petrophysical model showing the three Shajara Reservoir Units with their corresponding values of transverse relaxation time of nuclear magnetic resonance fractal dimension and capillary pressure fractal dimension

| Formation | Reservoir | Sample | Porosity % | k (md) | Positive slope of the first procedure Slope=3-Df | Negative slope of the second procedure Slope=Df-3 | Nuclear magnetic resonance fractal dimension | Capillary pressure fractal dimension |
|---------------------------------------|--------------------------|--------|------------|--------|--|---|--|--------------------------------------|
| Permo-Carboniferous Shajara Formation | Upper Shajara Reservoir | SJ13 | 25 | 973 | 0.2128 | -0.2128 | 2.7872 | 2.7872 |
| | | SJ12 | 28 | 1440 | 0.2141 | -0.2141 | 2.7859 | 2.7859 |
| | | SJ11 | 36 | 1197 | 0.2414 | -0.2414 | 2.7586 | 2.7586 |
| | Middle Shajara Reservoir | SJ9 | 31 | 1394 | 0.2214 | -0.2214 | 2.7786 | 2.7786 |
| | | SJ8 | 32 | 1344 | 0.2248 | -0.2248 | 2.7752 | 2.7752 |
| | | SJ7 | 35 | 1472 | 0.2317 | -0.2317 | 2.7683 | 2.7683 |
| | Lower Shajara Reservoir | SJ4 | 30 | 176 | 0.3157 | -0.3157 | 2.6843 | 2.6843 |
| | | SJ3 | 34 | 56 | 0.5621 | -0.5621 | 2.4379 | 2.4379 |
| | | SJ2 | 35 | 1955 | 0.2252 | -0.2252 | 2.7748 | 2.7748 |
| | | SJ1 | 29 | 1680 | 0.2141 | -0.2141 | 2.7859 | 2.7859 |

The Lower Shajara reservoir was denoted by six sandstone samples (Figure 1), four of which label as SJ1, SJ2, SJ3 and SJ4 were carefully chosen for capillary pressure measurement as established in Table 1. Their positive slopes of the first procedure log of the ratio of transverse relaxation time of nuclear magnetic resonance (NMRT2) to maximum transverse relaxation time of nuclear magnetic resonance (NMRT2max) versus log wetting phase saturation (S_w) and negative slopes of the second procedure log capillary pressure (P_c) versus log wetting phase saturation (S_w) are explained in Figure 2, Figure 3, Figure 4, Figure 5 and Table 1. Their transverse relaxation time of nuclear magnetic resonance fractal dimension and capillary pressure fractal dimension values are revealed in Table 1. As we proceed from sample SJ2 to SJ3 a pronounced reduction in permeability due to compaction was described from 1955 md to 56 md which reflects decrease in transverse relaxation time of nuclear magnetic resonance fractal dimension from 2.7748 to 2.4379 as quantified in table 1. Again, an increase in grain size and permeability was proved from sample SJ4 whose transverse relaxation time of nuclear magnetic resonance fractal dimension and capillary pressure fractal dimension was found to be 2.6843 as pronounced in Table 1.



Figure 1: Surface type section of the Shajara reservoirs of the Shajara Formation at latitude 26 52 17.4, longitude 43 36 18.

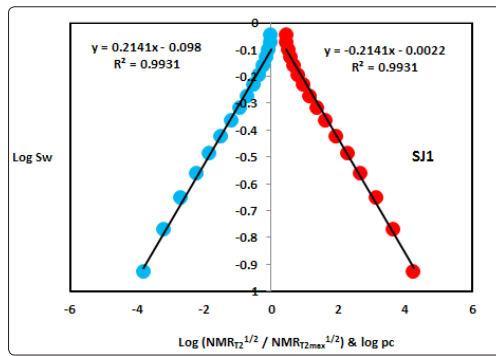


Figure 2: Log ($NMR_{12}^{1/2} / NMR_{12max}^{1/2}$) & log pc versus log Sw of sample SJ1

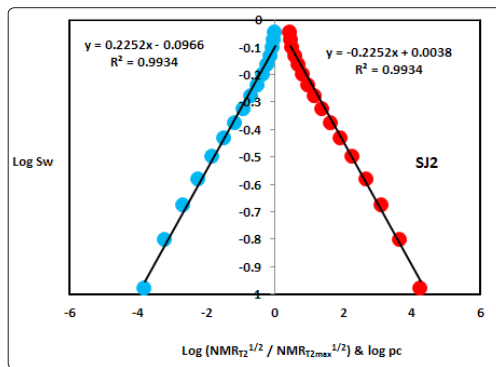


Figure 3: Log ($NMR_{12}^{1/2} / NMR_{12max}^{1/2}$) & log pc versus log Sw of sample SJ2

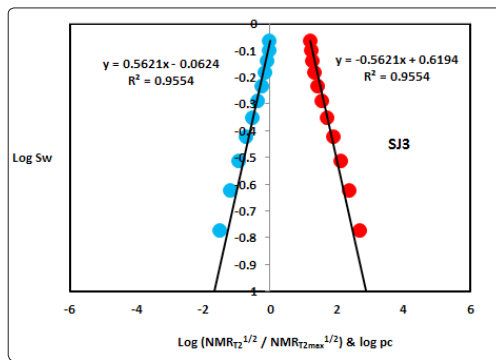


Figure 4: Log ($NMR_{12}^{1/2} / NMR_{12max}^{1/2}$) & log pc versus log Sw of sample SJ3

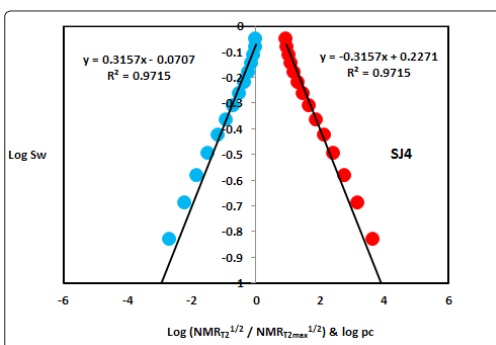


Figure 5: Log ($NMR_{12}^{1/2} / NMR_{12max}^{1/2}$) & log pc versus log Sw of sample SJ4

of sample SJ4

In contrast, the Middle Shajara reservoir which is separated from the Lower Shajara by an unconformity surface as shown in Figure 1. It was nominated by four samples (Figure 1), three of which named as SJ7, SJ8, and SJ9 as clarified in Table 1 were chosen for capillary measurements as described in Table 1. Their positive slopes of the first procedure and negative slopes of the second procedure are shown in Figure 6, Figure 7 and Figure 8 and Table 1. Furthermore, their transverse relaxation time of nuclear magnetic resonance fractal dimensions and capillary pressure fractal dimensions show similarities as defined in Table 1. Their fractal dimensions are higher than those of samples SJ3 and SJ4 from the Lower Shajara Reservoir due to an increase in their permeability as explained in table 1.

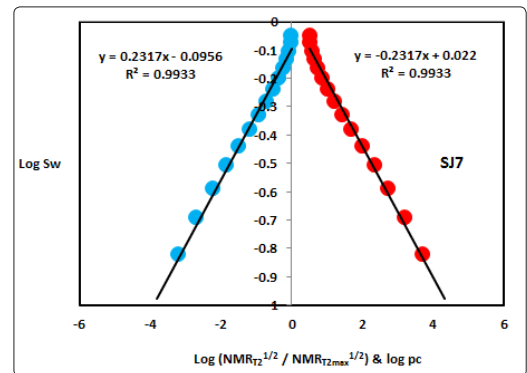


Figure 6: Log ($NMR_{12}^{1/2} / NMR_{12max}^{1/2}$) & log pc versus log Sw of sample SJ7

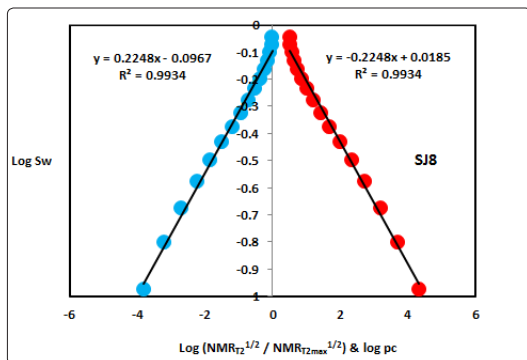


Figure 7: Log ($NMR_{12}^{1/2} / NMR_{12max}^{1/2}$) & log pc versus log Sw of sample SJ8

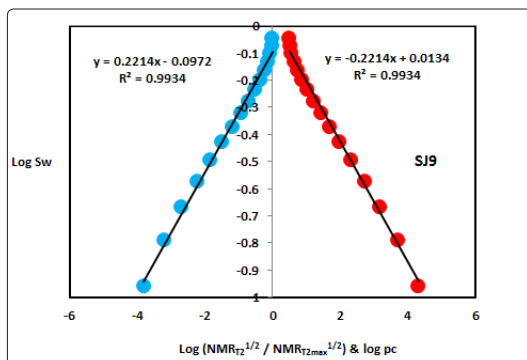


Figure 8: Log ($NMR_{12}^{1/2} / NMR_{12max}^{1/2}$) & log pc versus log Sw of sample SJ9

On the other hand, the Upper Shajara reservoir was separated from the Middle Shajara reservoir by yellow green mudstone as shown in Figure 1. It is defined by three samples so called SJ11, SJ12, SJ13 as explained in Table 1. Their positive slopes of the first procedure and negative slopes of the second procedure are displayed in Figure 9, Figure 10 and Figure 11 and Table 1. Moreover, their transverse relaxation time of nuclear magnetic resonance fractal dimension and capillary pressure fractal dimension are also higher than those of sample SJ3 and SJ4 from the Lower Shajara Reservoir due to an increase in their permeability as simplified in table 1.

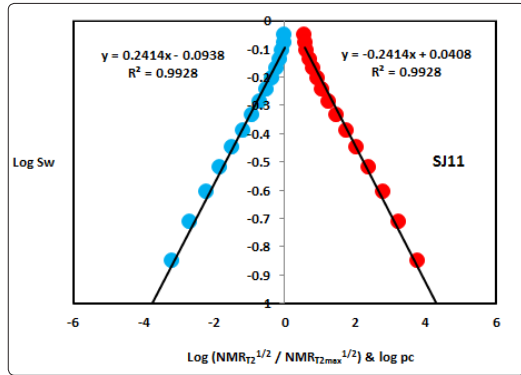


Figure 9: $\log (NMR_{T1}^{1/2} / NMR_{T2max}^{1/2})$ & $\log pc$ versus $\log Sw$ of sample SJ11

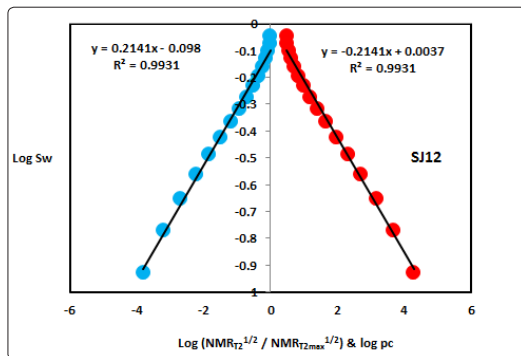


Figure 10: $\log (NMR_{T1}^{1/2} / NMR_{T2max}^{1/2})$ & $\log pc$ versus $\log Sw$ of sample SJ12

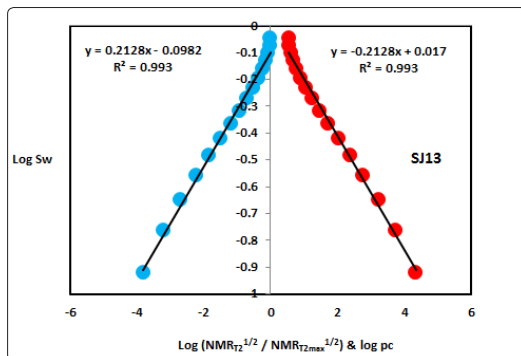


Figure 11: $\log (NMR_{T1}^{1/2} / NMR_{T2max}^{1/2})$ & $\log pc$ versus $\log Sw$ of sample SJ13

Overall a plot of positive slope of the first procedure versus negative slope of the second procedure as described in Figure 12 reveals three permeable zones of varying Petrophysical properties. These reservoir zones were also confirmed by plotting transverse relaxation time

of nuclear magnetic resonance fractal dimension versus capillary pressure fractal dimension as described in Figure 13. Such variation in fractal dimension can account for heterogeneity which is a key parameter in reservoir quality assessment.

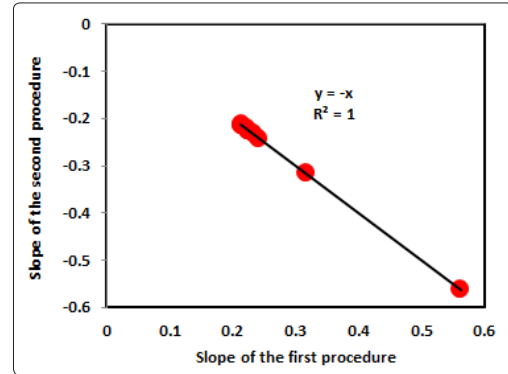


Figure 12: Slope of the first procedure versus slope of the second procedure

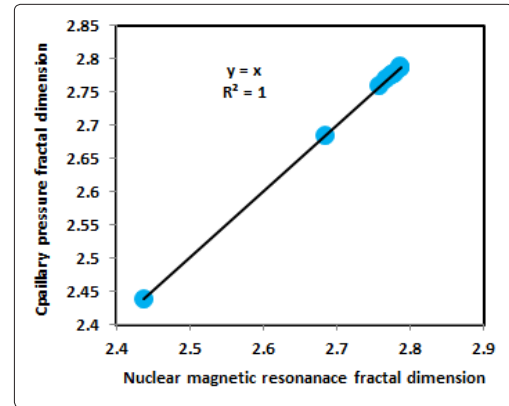


Figure 13: Nuclear magnetic resonance fractal dimension versus capillary pressure fractal dimension

Conclusion

- The sandstones of the Shajara Reservoirs of the Shajara formation permo-Carboniferous were divided here into three units based on transverse relaxation time of nuclear magnetic resonance fractal dimension.
- The Units from base to top are: Lower Shajara transverse relaxation time Nuclear Magnetic Resonance Fractal Dimension Unit, Middle Shajara Transverse Relaxation Time Nuclear Magnetic Resonance Fractal Dimension Unit, and Upper Shajara Transverse Relaxation Time Nuclear Magnetic resonance Fractal Dimension Unit.
- These units were also proved by capillary pressure fractal dimension.
- The fractal dimension was found to increase with increasing grain size and permeability owing to possibility of having interconnected channels.

Acknowledgement

The author would to thank King Saud University, college of Engineering, Department of Petroleum and Natural Gas Engineering, Department of Chemical Engineering, Research Centre at College of Engineering, and King Abdullah Institute for research and Consulting Studies for their supports.

References

1. Frenkel J (1944) On the theory of seismic and seismoelectric phenomena in a moist soil. *J physics* 3: 230-241.
2. Li K, Williams W (2007) Determination of capillary pressure function from resistivity data. *Transport in Porous Media* 67: 1-15.
3. Revil A, Jardani A (2010) Seismoelectric response of heavy oil reservoirs: theory and numerical modelling. *Geophysical J International* 180: 781-797.
4. Dukhin A, Goetz P, Thommes M (2010) Seismoelectric effect: a non-isochoric streaming current. 1 experiment. *J Colloid Interface Sci* 345: 547-553.
5. Guan W, Hu H, Wang Z (2012) Permeability inversion from low-frequency seismoelectric logs in fluid-saturated porous formations. *Geophysical Prospecting* 61: 120-133
6. Hu H, Guan W, Zhao W (2012) Theoretical studies of permeability inversion from seismoelectric logs. *Geophysical Research Abstracts*. 14: EGU2012-6725-1, 2012 EGU General Assembly 2012.
7. Borde C, S'en'echal P, Barri`ere J, Brito D, Normand in E et al. (2015) Impact of water saturation on seismoelectric transfer functions: a laboratory study of co-seismic phenomenon. *Geophysical J International* 200: 1317-1335.
8. Jardani A, Revil A (2015) Seismoelectric couplings in a poroelastic material containing two immiscible fluid phases. *Geophysical J International* 202: 850-870.
9. Holzhauser J, Brito D, Bordes C, Brun Y, Guatarbes B (2016) Experimental quantification of the seismoelectric transfer function and its dependence on conductivity and saturation in loose sand. *Geophys Prospect* 65: 1097-1120.
10. Rong P, Xing W, Rang D, Bo D, Chun L (2016) Experimental research on seismoelectric effects in sandstone. *Applied Geophysics* 13: 425-436.
11. Djuraev U, Jufar S, Vasant P (2017) Numerical Study of frequency-dependent seismoelectric coupling in partially-saturated porous media. *MATEC Web of Conferences* 87, 02001 (2017).
12. Alkhdid KEME (2017) Pressure head fractal dimension for characterizing Shajara Reservoirs of the Shajara Formation of the Permo-Carboniferous Unayzah Group, Saudi Arabia. *Arch Pet Environ Biotech* 2017: 1-7.
13. Alkhdid KEME (2018) Geometric relaxation time of induced polarization fractal dimension for characterizing Shajara Reservoirs of the Shajara Formation of the Permo-Carboniferous Unayzah Group, Saudi Arabia. *Sci fed J Petroleum* 2: 1-6.
14. Alkhdid KEME (2018) Geometric relaxation time of induced polarization fractal dimension for characterizing Shajara Reservoirs of the Shajara formation of the Permo-Carboniferous Unayzah Group-Permo. *Int J Pet and Res* 2: 105-108.
15. Alkhdid KEME (2018) Arithmetic relaxation time of induced polarization fractal dimension for characterizing Shajara Reservoirs of the Shajara Formation. *Nanosci and Nanotechnol* 1: 1-8.
16. Alkhdid KEME (2018) Seismo Electric field fractal dimension for characterizing Shajara Reservoirs of the Permo-Carboniferous Shajara Formation, Saudi Arabia. *Pet petro Chem Eng J* 2: 1-8.
17. Alkhdid KEME (2018). Seismo Electric field fractal dimension for characterizing Shajara Reservoirs of the Permo-Carboniferous Shajara Formation, Saudi Arabia. *Acad J Environ Sci*. 6: 113-120.
18. Alkhdid KEME (2018) Resistivity Fractal Dimension for Characterizing Shajara Reservoirs of the Permo Carboniferous Shajara Formation Saudi Arabia. *Recent Adv Petrochem Sci* 5: 1-6.
19. Alkhdid KEME (2018) Resistivity fractal dimension for characterizing Shajara reservoirs of the permo-carboniferous Shajara formation Saudi Arabia. *Int J Petrochem Sci Eng* 3: 109-112.
20. Alkhdid KEME (2018) Electro Kinetic Fractal Dimension for Characterizing Shajara Reservoirs of the Permo-Carboniferous Shajara Formation, Saudi Arabia. *Arch Oil Gas Res* 1: 1-7.
21. Alkhdid KEME (2018) Electro Kinetic Fractal Dimension for Characterizing Shajara Reservoirs of the Shajara Formation. *International Journal of Nanotechnology in Medicine and Engineering* 3: 1-7.
22. Alkhdid KEME (2018) Electric Potential Energy Fractal Dimension for Characterizing Permo-carboniferous Shajara Formation. *Expert Opin Environ Biol* 7: 1-5.
23. Alkhdid KEME (2018) Electric potential gradient Fractal Dimension for Characterizing Shajara Reservoirs of the Permo-Carboniferous Shajara Formation, Saudi Arabia. *Arch Petro Chem Eng* 1: 1-6.
24. Alkhdid KEME (2018) Seismic Time fractal dimension for characterizing Shajara reservoirs of the Permo-Carboniferous Shajara Formation, Saudi Arabia. *Mod App Ocean & Pet sci* 2: 1-6.

Copyright: ©2019 Prof. Khalid Elyas Mohamed Elameen Alkhdid. This is an open-access article distributed under the terms of the Creative Commons Attribution License, which permits unrestricted use, distribution, and reproduction in any medium, provided the original author and source are credited.